

# Accurate evaluation of the Green's function of disordered graphenes

W. Zhu<sup>1,2</sup>, Q. W. Shi<sup>1,2†</sup>, X. R. Wang<sup>2,3\*</sup>, X. P. Wang<sup>1</sup>, J. L. Yang<sup>1</sup>, J. Chen<sup>4,5</sup>, J. G. Hou<sup>1</sup>

<sup>1</sup>*Hefei National Laboratory for Physical Sciences at Microscale,  
University of Science and Technology of China, Hefei 230026, China*

<sup>2</sup>*Department of Physics, The Hong Kong University of Science and Technology,  
Clear Water Bay, Kowloon, Hong Kong*

<sup>3</sup>*School of Physics, Shangdong University, Jinan, P. R. China*

<sup>4</sup>*Electrical and Computer Engineering,  
University of Alberta, Alberta, Canada T6G 2V4 and*

<sup>5</sup>*National Research Council/National Institute  
for Nanotechnology, Alberta, Canada T6G 2M9\**

(Dated: May 21, 2010)

## Abstract

An accurate simulation of Green's function and self-energy function of non-interacting electrons in disordered graphenes are performed. Fundamental physical quantities such as the elastic relaxation time  $\tau_e$ , the phase velocity  $v_p$ , and the group velocity  $v_g$  are evaluated. New features around the Dirac point are revealed, showing hints that multi-scattering induced hybridization of Bloch states plays an important role in the vicinity of the Dirac point.

PACS numbers: 81.05.ue, 71.55.-i, 71.23.-k

---

\*Electronic address: phsqw@ustc.edu.cn; phxwan@ust.hk

*Introduction.* — Graphene, a single layer of graphite, has been intensively studied in recent years because of many intriguing transport properties [1, 2]. Examples include minimum conductivity and linear carrier density dependence of conductivity [3, 4]. Electrons in an ideal graphene are governed by the relativistic massless Dirac equation and exhibit a linear dispersion relation in the vicinity of the Dirac point and zero density of state at the Dirac point [5, 6]. Among many relativistic effects, the Klein paradox [7] is arguably one of the most important effects that differentiates Dirac electrons [8] from the Schrodinger electrons in disordered systems.

A deep understanding of Dirac electrons in disordered graphenes requires extended knowledge on the self-energy function in order to extract such fundamental physical quantities as the phase velocity  $v_p$ , the group velocity  $v_g$ , and the elastic relaxation time  $\tau_e$ . However, it is known [9] that accurate and reliable calculations are quite difficult and nontrivial. For this reason, various approximations have been employed in different theoretical studies. So far, almost all calculations [10, 11] concerning electron properties in disordered graphenes were performed without fully considering disorder effects. The wave-nature of Dirac electrons is more pronounced near the Dirac point because of very large electron wavelength there. It is known that interference due to multi-scattering leads to weak localization and the Anderson localization in conventional disordered electron systems[12]. Quantum interference also plays important roles in coherent wave propagation through quasi-random [13] and random media[14, 15]. As it will be shown below, interference-induced the hybridization of Bloch states is essential in understanding the diffusion properties near the Dirac point in realistic disordered graphenes, although previous calculations [10, 11] only captured the essential physics far away from the Dirac point.

In this Letter, we present a systematic method to exactly calculate Green's function and the self-energy of large size disordered graphenes. We extract accurate  $\tau_e$ ,  $v_p$ , and  $v_g$  values from the spectral function  $A(\mathbf{k}, E)$  derived from the self-energy function. In comparison with the results from the self-consistent Born approximation (SCBA), it is found that  $\tau_e$  is overestimated by the SCBA in the strong disorder regime. We show that both  $v_p$  and  $v_g$  deviate significantly from their unrenormalized values and exhibit substantial energy dependence, especially near the Dirac point. The effective group velocity is larger than the effective phase velocity, but significantly lower than its unrenormalized value when the mixing of different Bloch states is dominant. Moreover, we generalize the Einstein relation

to calculate the conductivity of the disordered graphene.

*Model-and-method.* –  $\pi$ -electrons of undoped graphene can be modeled by a tight-binding Hamiltonian on a honeycomb lattice of two sites per unit cell,  $H_0 = t \sum_{\langle ij \rangle} |i\rangle \langle j| + h.c.$ , where  $t = -2.7$  eV is the hopping energy. The corresponding eigenvalues and eigenstates of  $H_0$  near the Dirac point are [5, 17], respectively,  $E_{k,\pm} = \pm \hbar v_F^0 k$  and  $|\mathbf{k}\pm\rangle = (|\mathbf{k}A\rangle \pm e^{i\phi(\mathbf{k})} |\mathbf{k}B\rangle)/2$ , where  $v_F^0$  is the unrenormalized Fermi velocity, and  $\hbar$  is the Plank constant.  $A$  and  $B$  stand for  $A$ - and  $B$ -sublattices.  $\phi(\mathbf{k})$  is the polar angle of the momentum  $\mathbf{k}$ , and  $|\mathbf{k}A(B)\rangle = \frac{1}{\sqrt{N_{A(B)}}} \sum_{\mathbf{r}_{A(B)}} e^{i\mathbf{k}\cdot\mathbf{r}_{A(B)}} |\mathbf{r}_{A(B)}\rangle$ , where  $\mathbf{r}_{A(B)}$  is the position vector of the  $A(B)$ -lattice and  $N_{A(B)}$  is the total  $A(B)$ -lattice points. The plus (minus) sign denotes the conduction (valence) band. The Green function of clean graphene is, in a diagonal basis,  $G_0(\mathbf{k}, E) = \frac{1}{E+i0^+ - \hbar v_F^0 k} |\mathbf{k}+\rangle \langle \mathbf{k}+| + \frac{1}{E+i0^+ + \hbar v_F^0 k} |\mathbf{k}-\rangle \langle \mathbf{k}-|$ . A weak point-like disorder is introduced through  $V = \sum \epsilon_i |i\rangle \langle i|$  with  $n_{imp}$  randomly distributed impurity sites where the on-site energy  $\epsilon_i$  of each impurity can take  $-V_0$  or  $V_0$  (measured in the unit of  $t$ ) with equal probability. A dimensionless parameter  $\alpha = \frac{n_{imp} V_0^2 A_c}{2\pi (\hbar v_F^0)^2}$  can be used to characterize disorder strength. Here,  $A_c$  is the area of the unit cell. Our calculation shows that the physical quantities such as self-energy are only determined by the parameter  $\alpha$  [18].

The ensemble-averaged Green function is defined as  $G(\mathbf{k}\pm, E) = \overline{\langle \mathbf{k}\pm | \frac{1}{E+i\eta - H_0 - V} | \mathbf{k}\pm \rangle}$ , where the bar means the ensemble average. It can be calculated by using the well developed Lanczos recursive method [19, 20]. In order to obtain an accurate ensemble-averaged Green's function near the Dirac point with high energy resolution [21], a large sample containing  $N = L_x \times L_y \simeq 6.0$  millions carbon atoms ( $2400 \times 2400$ ) is used in our simulation, where  $L_x(L_y)$  is the number of atoms in  $x(y)$  directions. The periodic boundary condition is used in our simulation in order to reduce the finite size effect. Thus, the wave vectors are  $k_x = n_x 4\pi / 3aL_x$  and  $k_y = n_y 4\pi / \sqrt{3}aL_y$ , where  $n_{x(y)}$  is an integer and  $a$  is the lattice constant.

*Self-energy function.* – Fig. 1 shows the calculated real (a) and imaginary (b) parts of the self-energy function for  $n_{imp}/N = 10\%$  and  $V_0 = 0.5$  (open squares) and  $2.0$  (open circles), respectively. The self-energy function is defined as usual, where  $\Sigma(\mathbf{k}, E) = G_0^{-1}(\mathbf{k}, E) - G^{-1}(\mathbf{k}, E)$  [23]. In principle, the self-energy function depends on energy  $E$  and wave vector  $\mathbf{k}$ . However, our simulation finds that the self-energy function is not sensitive to wave vector  $\mathbf{k}$ , while the one-particle Green's function depends on both  $E$  and  $\mathbf{k}$ . This is not surprising

since the scatterer size is much smaller than the electron wavelength near the Dirac point so that the inhomogeneous structure of disordered graphene can be described well by an effective homogeneous medium. This is also why the self-energy function is assumed to be  $\mathbf{k}$ -independent in many perturbative calculations. Our finding validates this assumption[23].

Our calculation should be compared with widely used results from the self-consistent Born approximation (SCBA) that predicts [17, 24]

$$\Sigma(E) = \begin{cases} -2E/\alpha - i2\Gamma_0, & |E| \ll \Gamma_0 \\ -2\alpha(E + i\pi\alpha|E|)\ln|\frac{E_c}{E}| - i\pi\alpha|E|, & |E| \gg \Gamma_0 \end{cases}$$

where  $\Gamma_0 = E_c e^{-1/\alpha}$  ( $E_c$  is the cut-off energy) As shown in Fig. 1, SCBA results agree well with our exact self-energy function for very weak disorder ( $V_0=0.5$  and  $n_{imp}/N=10\%$ )[25]. When the disorder strength increases several times ( $V_0=2.0$  or  $\alpha\sim 0.07$ ), the perturbative results can not capture the main features, especially near the Dirac point. The discrepancy is obvious for  $Im\Sigma(0)$  as shown in Fig. 1(b).  $Im\Sigma(E)$  at the Dirac point is  $\Gamma_0 \sim 10^{-5}t$  ( $E_c = \sqrt{3}t$  [6]) from the SCBA, while our exact value is  $Im\Sigma(0) \sim 10^{-2}t$ . Thus, the true broadening of states at or near the Dirac point is much greater than what has been predicted by SCBA. This huge discrepancy can be attributed to the mixture of Bloch states caused by the impurities. Furthermore, the level-repulsion effect pushes all energy level toward the Dirac point so that the density of states at the Dirac point increases more in the presence of impurities. Thus, the impurities make the imaginary part of the self-energy function (directly associated with the density of states) at the Dirac point bigger. When the wavelength becomes short and the quantum interference as well as the Bloch state mixing are less important,  $Im\Sigma(E)$  are determined by the disorder scattering. The difference between our exact simulation and that of the SCBA is small as shown in Fig. 1.

*Spectral function.* – The single-particle spectral function relates to Green's function through  $A(\mathbf{k}\pm, E) = -ImG(\mathbf{k}\pm, E)/\pi$ . Fig. 2(a) is  $A(\mathbf{k}+, E)$  for  $k_y = 0$ ,  $V_0 = 1$ ,  $n_{imp}/N=10\%$ , and various  $k_x$  (curves from the left to the right in the figure) ranging from 0.0 ( $n_x=0$ ) to 0.098 ( $n_x=56$ ) (in unit of  $a^{-1}$ ). In the absence of disorder, the spectral function  $A_0(\mathbf{k}\pm, E)$  is a delta function, reflecting that the wave vector  $\mathbf{k}$  is a good quantum number and has all its spectral weight precisely at the energy  $E = E_{k\pm}$ . In the presence of disorder, the translational symmetry is broken and the spectral function is broadened due to the disorder scattering effect. The widths of the spectral function are given by  $Im\Sigma(E)$

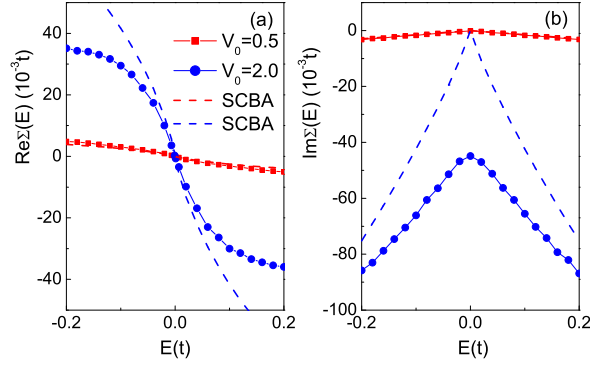


FIG. 1: (Color online) (a) Real part of self-energy as a function of energy. (b) Imaginary part of self-energy as a function of energy. The open squares and open circles represent our numerical calculations for the disorder concentration  $n_{imp}/N = 10\%$  and  $V_0 = 0.5$  and  $V_0 = 2.0$ , respectively. Dashed lines represent the SCBA results for the same disorder. Energy is measured in the units of  $t$ .

that measures the elastic relaxation lifetime  $\tau_e$ , where  $\tau_e = \frac{\hbar}{-2\text{Im}\Sigma(E)}$ . Therefore, the elastic scattering relaxation time is akin to  $\text{Im}\Sigma(E)$ , and  $\tau_e$  around the Dirac point is mainly determined by the Bloch state mixing and the level repulsion effect[26]. Far away from the Dirac point, the lifetime is mainly attributed to the disorder scattering. As shown in the inset of Fig. 2, lifetime become shorter as the wave vector increases. Physically, this is because the density of states  $\rho$  increases linearly with energy and the disorder scattering effects become larger, which is qualitatively consistent with the prediction of SCBA[16, 17, 24].

*Effective band velocity.* – Dirac electron propagation velocities, including the group velocity  $v_g$  and phase velocity  $v_p$ , are also greatly modified by the disorder effects. These quantities relate to the shape of the dispersion relation that is the roots of  $E - E_0(k) - \text{Re}\Sigma(E) = 0$ [27, 28]. One can also extract the dispersion relation from the peak of the spectral function  $A(\mathbf{k}, E)$  for a given  $\mathbf{k}$ . Fig 3 (a) shows our exact dissipation curve  $E_{eff}(k)$  that is linear for very weak disorder ( $\alpha < 0.01$ ). However, when the disorder strength becomes significantly large ( $\alpha \sim 0.1$ ), the  $E_{eff}(k)$  becomes concave near the Dirac point, indicating the reduction in both the group and phase velocities.

Fig. 3(b) shows  $k$ -dependence of the group and phase velocities obtained from  $v_g = \partial E_{eff}(k)/\partial k$  and  $v_p = E_{eff}/k$ . For the very weak disorder  $\alpha = 0.01$  as shown in the figure,

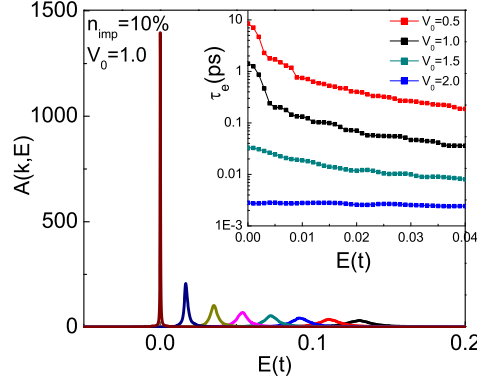


FIG. 2: (Color online) Single-particle spectral function  $A(\vec{k}+, E)$  plotted as a function of energy  $E$  at several  $k$ -points (from left to right):  $k = 0.000, 0.014, 0.028, 0.042, 0.056, 0.070, 0.084, 0.098$  (or  $n_x = 0 \sim 56$ ) along the  $k_x$  direction. The model parameters are  $n_{imp}/N = 10\%$  and  $V_0 = 1.0$ . Inset: The energy dependence of single-particle relaxation time  $\tau_e$  for  $V_0 = 0.5 \sim 2.0$  and  $n_{imp}/N = 10\%$ .

$v_g$  and  $v_p$  are not too much different from the unrenormalized velocity  $v_F^0$ . Their values are reduced by 5% in comparison with  $v_F^0$ . When the disorder strength increase several times  $\alpha = 0.07$ , the renormalized  $v_g$  is higher than  $v_p$  and both  $v_g$  and  $v_p$  are reduced by a large percentage near the Dirac point. This shows that disorder not only renormalizes the Dirac electron velocities, but also changes the linear dispersion relation. The fact of large reductions of velocities at the Dirac point indicates that Dirac electrons near the Dirac point are more sensitive to the disorder.

One can use the renormalization factor  $Z$  defined as  $Z = (1 - \frac{\partial \text{Re}\Sigma(E, \mathbf{k})}{\partial E})^{-1}$  [29] to measure the effect of disorder on electronic structure. Its value equals the ratio  $v_g/v_F^0$ . As shown in Fig. 3(b),  $Z$  is very close to 1.0 for very weak disorder. In this regime, the Bloch state is still a good starting point for understanding disordered graphene, while the transport properties are expected to be described by the quasi-classical Boltzmann theory. When the disorder strength increases several times, calculations shows that  $Z$  is much smaller than 1.0, especially around the Dirac point. This unusual feature directly reflects that a Bloch states around the Dirac point couples strongly with other nearby Bloch states. Therefore, the Bloch states would not be a good starting point to perform perturbative calculations. In fact, the similar feature has been observed in semiconductor alloys and has been termed non-Bloch nature of alloy states[30]. This is why the SCBA method cannot produce accurate enough

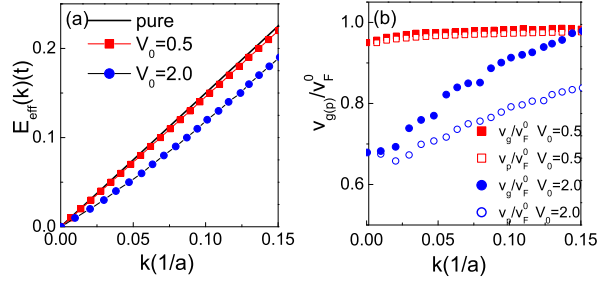


FIG. 3: (Color online) (a) Effective energy dispersion relation for ideal graphene and disordered graphenes for  $n_{\text{imp}}/N = 10\%$  and  $V = 0.5$  (filled squares) and  $V = 2.0$  (filled circles). (b) The ratio  $v_g/v_F^0$  (filled symbols) and  $v_p/v_F^0$  (open symbols) as a function of wavenumber  $k$  (in units of  $1/a$ ).

results. This nontrivial feature could lead to intriguing transport and optical properties. For example, linear dispersion relation leads to  $E_n = \pm v_F^0 \sqrt{2e\hbar n B}$  ( $n = 0, 1, 2, \dots$ ) LL series. Since the LLs come from the quench of electron's kinetic energies, lower group velocity near the Dirac point means the energy gap between  $n = 0$  LL and  $n = \pm 1$  LL should be substantially reduced by the disorders while that between  $n = \pm 1$  LLs and  $n = \pm 2$  LLs will be affected less by disorder. As a result, one should expect the ratio  $(E_2 - E_{-1})/(E_1 - E_0)$  is substantially larger than  $\sqrt{2} + 1$ . This is indeed what was observed in a recent experiment[31] where  $(E_2 - E_{-1})/(E_1 - E_0)$  is found to be greater than  $\sqrt{2} + 1$ , by  $5 \sim 10\%$ . This observation implies that their samples are quite disordered.

*Conductivity.* – Assuming that the Einstein relation for the Dirac electrons is valid, one can obtain the conductivity from  $\sigma = e^2 D \rho$ , where  $e$  is the electron charge,  $D = v_g^2 \tau_{tr}/2$  is the diffusion coefficient, and  $\tau_{tr}$  denotes the transport relaxation time and satisfies the relationship  $\tau_{tr} = 2\tau_e$  for the point-like disorder. [17] Fig. 4 is the conductivity calculated from transport relaxation time  $\tau_{tr} = 2\tau_e$  in Fig. 2, the group velocity  $v_g$  in Fig. 3, and the density of states obtained by  $\rho(E) = -\frac{A_c}{\pi} \int_0^{k_c} \frac{d\vec{k}}{(2\pi)^2} A(\vec{k}, E)$  as shown in inset to Fig. 4. For very weak disorder, the conductivity is sub-linear in the Fermi energy. Increasing the disorder strength, the conductivity weakly depends on the Fermi energy or the carrier density, in agreement with the prediction of Boltzmann theory for short-range scatterers [17]. At the Dirac point, by combining the self-energy function with Kubo formula, the conductivity is predicted to have the universal value  $\sigma_{xx}(0) = 4e^2/\pi\hbar$ [32]. However, our

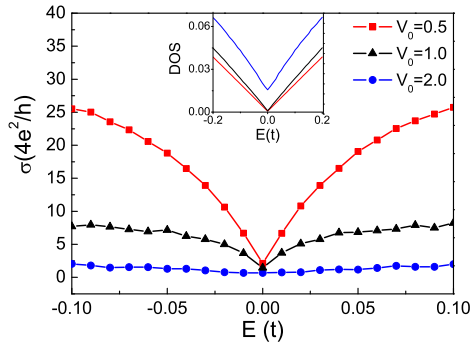


FIG. 4: (Color online) Conductivity as a function of charge density. The model parameters are  $n_{imp}/N = 10\%$  and  $V_0 = 0.5, 1.0$  and  $2.0$ . Inset: Density of states for the same parameters.

calculations find that  $\sigma_{xx}(0)$  takes the values  $8.2e^2/h$ ,  $5.9e^2/h$  and  $2.7e^2/h$  for  $\alpha = 0.0046$ ,  $0.018$  and  $0.07$ , respectively, and shows non-universal behavior.

*Summary.* — In conclusion, we studied point-like disorder effects on the one-electron properties of graphene. The exact ensemble-averaged Green's function is obtained from a large-scale real-space calculation. Through the analysis of self-energy and spectral functions, we conclude that the single-particle lifetime reduction and the linear dispersion relation are modified by the hybridization of the Bloch states. Furthermore, we studied the diffusion transport properties by using our exact self-energy and the Einstein relation. Our approach is very general and robust, thus is applicable to many other disordered systems.

*Acknowledgment.*— This work is partially supported by NNSF of China (Nos. 10974187, 10874165, and 50721091), by NKBRP of China under Grant No. 2006CB922000, and by KIP of the Chinese Academy of Sciences (No. KJCX2-YW-W22). JC is supported by the NRC and NSERC of Canada (No. 245680). XRW acknowledges the support of Hong Kong RGC grants (#604109, RPC07/08.SC03, and HKU10/CRF/08-HKUST17/CRF/08).

- 
- [1] K. S. Novoselov, *et. al*, Science 306, 666 (2004)
  - [2] Y. Zhang, *et. al*, Nature, 438, 201 (2005).
  - [3] A. K. Geim, *et. al*, Nat. Mater. 6, 183 (2007).
  - [4] S. Das Sarma, *et. al*, Solid State Commun. 143, 1(2007).
  - [5] A. H. Castro Neto, *et. al*, Rev. Mod. Phys. 81,109 (2009).



- [6] Z.F. Wang, *et. al*, Phys. Rev. B, 74, 125417(2006).
- [7] M. Katsnelson, K. Novoselov, and A. Geim, Nat. Phys. 2, 620 (2006).
- [8] Y.Y. Zhang, *et. al*, Phys. Rev. Lett. 102, 106401 (2009); Phys. Rev. B 78, 155413 (2008).
- [9] E. N. Economou, *Green's Functions in Quantum Physics*, Springer (2006).
- [10] E. H. Hwang and S. Das Sarma, Phys. Rev. B, 77, 195412 (2008).
- [11] M. I. Katsnelson, *et. al*, Phil. Trans. R. Soc. A 366, 195(2008).
- [12] P. A. Lee, *et. al*, Rev. Mod. Phys. 57, 287 (1985).
- [13] X. R. Wang, Phys. Rev. B 51, 9310 (1995); 53, 12035 (1996).
- [14] M. C. W. van Rossum, *et. al*, Rev. Mod. Phys. 71, 313 (1999).
- [15] M. P. van Albada, *et. al*, Phys. Rev. Lett. 66, 3132 (1991).
- [16] K. Normura and A. H. MacDonald, *ibid.* 96, 256602 (2006); *ibid.* 98, 076602 (2007).
- [17] T. Ando, J. Phys. Soc. Jpn. 75, 074716 (2006); N. H. Shon and T. Ando, J. Phys. Soc. Jpn. 67, 2421 (1998).
- [18] Other uncorrelated short range impurity potential (such as Anderson disorder) produces similar results.
- [19] J. K. Cullum and R. A. Willoughby, *Lanczos Algorithms for large symmetric eigenvalue problem*, Birkhauser(1985); C. Lanczos, J. Res. Natl. Bur. Stand. 45, 255 (1950); R. Haydock, V. Heine, and M. J. Kelly, J. Phys. C 5, 2845 (1972); S. D. Wu, *et al.*, Phys. Rev. B 77, 195411 (2008).
- [20] E. Dagotto, Rev. Mod. Phys. 66, 763 (1994); L. C. Davis, Phys. Rev. B 28, 6961 (1983); B. Bauml, *et.al ibid.* 58, 3663 (1998); S. M. Anaage, *et.al, ibid.* 34, 2336 (1998).
- [21] A small artificial cut-off energy  $\eta$  is used to simulate the infinitesimal imaginary energy in Green function. This artificial cut-off energy may be viewed as a measure of electron-phonon or electron-electron interactions in reality. We chose  $\eta = 0.01meV$  in this paper, which is much less than the energy resolution in recent ARPES experiments [22]. See also W. Zhu *et.al*, Phys. Rev. Lett. 102, 056803 (2009).
- [22] A. Damascelli, *et. al*, Rev. Mod. Phys. 75, 473(2003).
- [23] A. Altland and B. Simons, *Condensed Matter Field Theory*, Cambridge (2006).
- [24] P. M. Ostrosky, *et. al*, Phys. Rev. B 74, 235443(2006).
- [25] T. Fukuzawa, *et. al*, J. Phys. Soc. Jpn. 78, 094714(2009).
- [26] M. Calandra and F. Mauri, Phys. Rev. B 76, 205411 (2007).

- [27] G. D. Mahan, *Many-Particle Physics*, third edition, Kluwer Academic, New York (2000).
- [28] K. Tarafder, *et. al*, Phys. Rev. B 74, 144204 (2006).
- [29] C. H. Park, *et. al*, Phys. Rev. Lett. 99, 086804 (2007).
- [30] L.-W. Wang, *et. al*, *ibid.* 80, 4725(1997); Y. Zhang, *et. al*, *ibid.* 101, 036403 (2008).
- [31] E.A. Henriksen, *et. al*, *ibid.* 104, 067404 (2010); E.A. Henriksen (private communication).
- [32] T. Ando, *et. al*, J. Phys. Soc. Jpn. 71, 1318 (2002).